HYDROTHERMAL SYNTHESIS OF ALUMINA/SILICA HYBRID MATERIALS AND THEIR APPLICATION ON LYOCELL FABRICS

MING-SHIEN YEN, MU-CHENG KUO, CHIEN-WEN CHEN and YEN-SHENG CHENG

Department of Materials Engineering, Kun Shan University, Tainan 71003, Taiwan, Republic of China
✉ *Corresponding author: Ming-Shien Yen, yms0410@mail.ksu.edu.tw*

Received June 24, 2015

A series of novel alumina/silica hybrid materials were prepared via the hydrothermal process from aluminum isopropoxide (AIP), methyltrimethoxysilane (MTMS), and n-octyltriethoxysilane (OTES). The structures of the alumina/silica hybrid materials were characterized using Fourier transform infrared (FTIR) analysis and ^{27}Al and ^{29}Si nuclear magnetic resonance (NMR) imaging. Gray Lyocell fabrics were first dyed and then coated with the alumina/silica hybrid materials through a padding–drying–thermosol process. The bonding structures of the treated Lyocell fabrics were evaluated using scanning electron microscopy (SEM) and energy dispersive X-ray spectroscopy (EDS) analyses. The evenness of the coated layer on the Lyocell fabrics was confirmed by SEM images, and the interaction of the hybrid materials with the Lyocell fabrics was verified. Moreover, water repellency and conductivity analyses of the treated fabrics were conducted. Our data show that the conductivity of the Lyocell fabrics treated with the alumina/silica hybrid materials was improved with increasing concentrations of aluminum isopropoxide in the reaction mixture. After modification with alumina/silica hybrid materials, all the treated Lyocell fabrics revealed good water repellency abilities.

Keywords: alumina, silica, Lyocell fabrics, hydrothermal, conductivity, water repellency

INTRODUCTION

Lyocell fiber has all the advantages of regenerated cellulose fibers: it has high strength in both wet and dry states, high absorbency, and it is fully biodegradable and easily processed. Lyocell fiber is produced by dissolving wood pulp in a solution of hot N-methyl morpholine N-oxide (NMMO) and then spinning the solution into fibers.[1,2] Lyocell material was developed to meet the demand for an environmentally friendly process to produce man-made cellulosic biodegradable fibers with improved cost and performance.[3] The unique properties of Lyocell, *i.e.*, high strength, excellent fabric and garment stability in the wet state, good dyeability with brilliant shades, and comfortable skin sensory properties, have led to the successful application of Lyocell for commercial products.[4-6]

Traditional (single-function) materials have been gradually replaced by multifunctional eco-friendly materials that can improve human health and add value to products.[7-10] Inorganic–organic composite materials with well-defined nanostructures have gained interest due to their improved properties resulting from the combination of two components in one uniform material.[11] As the inorganic component of hybrid inorganic–organic materials, alumina sol is used for a wide variety of purposes, and it can be produced as transparent alumina monoliths, alumina fibers, alumina films, and coatings[12-14] on various materials. Alumina sol is prepared mainly through one of two sol–gel methods. Yoldas[15] used aluminum alkoxide as a starting reagent, whereas Kurokawa[16] used an aluminum inorganic salt as a starting reagent. Alumina sol from inorganic salts is not as pure as that from alkoxide because of the ease with which impurities can be introduced. The majority of work on sol–gel processes uses

alkoxides as precursors.

Furthermore, silica is a natural material derived from common materials, such as quartz, sand, and flint. It has high chemical stability, a low thermal expansion coefficient, and high heat-resistance characteristics. The relatively high chemical stability of the silica phase can be advantageous in some cases.[17-20] Khatib's use of silica membranes for a hydrogen separation application reveals that silica-based membranes have emerged as promising materials at high temperatures owing to their high permeation rates, high selectivity, hydrothermal stability, resistance to poisons, and mechanical strength.[21]

The hydrothermal method provides advantages such as direct crystallization under hydrothermal conditions without sintering, regular morphology, uniform grain size, lower agglomeration, *etc*., it is widely used for the preparation of nanoparticles. It is also used in the preparation of hybrid materials that possess both the flexible performance of organic materials and the anti-friction, resistance to aging, and weathering characteristics of inorganic materials.[22-25] The modification of inorganic–organic materials greatly improves the surface properties of the organic material and expands its application.[26-29] Mousavand found that boehmite sol could be prepared by the hydrothermal method through hydrolysis in alcohol to achieve a film with microporous structure.[30]

This study adopted the hydrothermal method to synthesize a series of composite materials of aluminum isopropoxide sol hybrids, with methyltrimethoxysilane (MTMS) and n-octyltriethoxysilane (OTES) as chemical precursors. Various molar ratios of the alumina/silica hybrid materials were used to generate the network structures, and the chemical and physical properties of the treated Lyocell fabrics were evaluated. Water repellence, conductivity, and color fastness were analyzed to evaluate the physical properties of the treated Lyocell fabrics and to identify multifunctional benefits.

EXPERIMENTAL

Materials

Milled, scoured and bleached plain weave Lyocell fabrics [ends (94)*picks (58)/(20^s/1)*(20^s/1)] were supplied by Everest Textile Industry Co., Ltd., Tainan, Taiwan. MTMS, OTES and aluminum isopropoxide (AIP) were purchased from Acros Co., Ltd., Geel, Belgium. Sodium sulfate and sodium carbonate were purchased from Hayashi Pure Chemical Co., Ltd., Osaka, Japan. The reactive dye (C.I. reactive blue 19) was supplied by Everlight Chemical Industrial Co., Ltd., Taipei, Taiwan. The scouring agent laundry detergent (Lipofol TM-1000E) was supplied by Taiwan Nicca Chemical Industrial Co., Ltd., Taipei, Taiwan.

Preparation and processing

Dyeing of Lyocell fabrics

Lyocell fabrics were dyed using an infrared dyeing machine (LOGIC ART, LA-650) at a liquor ratio of 1:40 with distilled water. The dyeing bath was prepared with a reactive dye concentration of 2% on mass of fiber (o.m.f.), 20 g/L of sodium sulfate, and 10 g/L of sodium carbonate. Dyeing began at 30 °C for 10 min, and then the dye bath temperature was increased at a rate of 2 °C/min to 60 °C and maintained at this temperature for 40 min, followed by cooling to 40 °C. After dyeing, the fabrics were placed in a 2 g/L scouring agent liquor at 80 °C for 20 minutes for two washings and then dried at room temperature.

Preparation of hybrid materials

For the alumina synthesis, the alumina sol solution derived from aluminum isopropoxide, [$Al(OCH_3i)_3$], was prepared according to the method reported by Yoldas.[25] The [$Al(OCH_3i)_3$] was hydrolyzed in an excess of deionized water [$n H_2O$:$n Al(OCH_3i)_3$ = 100:1] for 1 h under vigorous stirring at 80 °C. Peptization was initiated by adding HNO_3, [$n Al(OCH_3i)_3$:$n HNO_3$ = 1:0.1] and the resulting colloidal suspension was refluxed for approximately 16 h under vigorous stirring at 80 °C, producing a viscous alumina sol solution. Then, constant ratios of MTMS and OTES were prepared, respectively, with 50 mL of deionized water and 5 mL of 99% ethanol. To complete the silica solution, the pH of the mixture was adjusted to 3.5 by adding 2 N hydrochloric acid at 40 °C with vigorous stirring for 30 min. Hybrid materials S_1–S_4 were synthesized using AIP:MTMS:OTES molar ratios of 1:2:0.5, 1:2:1, 1:2:2, and 1:2:3 (*i.e*., varying OTES amounts) in a clave hydrothermal instrument for 8 h. Hybrid materials P_1–P_4 were

synthesized using AIP:MTMS:OTES molar ratios of 0.5:2:2, 1:2:2, 1.5:2:2 and 2:2:2 (*i.e.*, varying AIP amounts) in the clave hydrothermal instrument for 8 h. The compositions of hybrid materials S_1–S_4 and P_1–P_4 are given in Table 1.

Table 1
Composition of S_1–S_4 and P_1–P_4

Compd.	AlOOH/MTMS/OTES	Compd.	AlOOH/MTMS/OTES
S_1	1:2:0.5	P_1	0.5:2:2
S_2	1:2:1	P_2	1:2:2
S_3	1:2:2	P_3	1.5:2:2
S_4	1:2:3	P_4	2:2:2

Treating Lyocell fabrics

The treatment of the Lyocell fabrics was performed using the "two dips, two nips" padding method with a pickup of 80%. A typical padding solution was prepared as follows: fabrics were dipped for 3 min in a sol solution containing the required weight percent of hybrid materials. A padding–drying–curing finishing procedure was used to disaggregate the agglomerated particles into well-dispersed colloidal particles. Fumed alumina and silica sol-treated fabric samples were padded and nipped to remove excess liquid and to obtain a percent wet pickup of 80% using a padder (Rapid Labortex Co., Ltd., Taoyuan, Taiwan) with a set nipping pressure. The treated fabric was pre-dried in an oven at 70 °C for 5 min. Then, the treated fabrics were cured at 100 °C for 90 s in a preheated curing oven (R3, Chang Yang Machinery Co., Taiwan). The treated fabrics were rinsed with water several times to thoroughly remove any hybrid material residue and dried at 70 °C for 5 min prior to analysis. The labels LS_1–LS_4 and LP_1–LP_4 denote the dyed Lyocell fabrics treated with hybrid materials S_1–S_4 and P_1–P_4, respectively.

Methods and characterization

Fourier transform infrared (FTIR) spectra were recorded on a Bio-Red Digilab FTS-40 spectrometer (KBr). The ^{27}Al and ^{29}Si nuclear magnetic resonance (NMR) spectra were collected using a Bruker Avance 400 MHz NMR spectrometer at 78.49 MHz with a recycle time of 60 s; the number of scans was 914. The surface morphology of the treated Lyocell fabrics was investigated using a field-emission scanning electron microscope (FE-SEM, Philips XL40). The color strength and evenness of the treated textiles were measured using a Hunter Lab Corporation spectrocolorimeter (MiniScan XE Plus/Color Flex, 4000S, D/8). Water contact angle measurements were made with a water contact angle meter (Sigma CAM100). The washing fastness was evaluated by the AATCC Test Method 61-2001 Test No. 2A using an AATCC Standard Instrumental Logic Art LA-650 Infrared Dyer. The conductivity of the treated Lyocell fabrics was analyzed using a high-impedance meter (MCP HT450, Mitsubishi). The operating voltage was 10 V with a test time of 1 min.

Determination of color strength and related parameters

The reflectance values of the treated samples were measured using an ultraviolet-visible (UV-Vis) spectrophotometer (UV-1201, Shimadzu) at λmax. K/S values were determined using the Kubelka-Munk equation:[31]

$$\frac{K}{S} = \frac{(1 - R_{\lambda max})^2}{2R_{\lambda max}} \quad (1)$$

where K is the coefficient of absorption, S is the coefficient of scattering, and $R_{\lambda max}$ is the reflectance value of the fabric at peak wavelength.

The color differences and relative color strengths of the fabrics coated with silica hybrid materials and of uncoated fabrics were obtained using the following relationships:

$$\text{Relative color strength (\%)} = \frac{K/S \text{ of treated sample}}{K/S \text{ of untreated sample}} \times 100\% \quad (2)$$

$$\Delta E = \sqrt{(\Delta L)^2 + (\Delta a)^2 + (\Delta b)^2} \quad (3)$$

where L is the lightness or shade of the dye, a is a measure of redness or greenness, and b is a measure of yellowness or blueness. It is noted that $\Delta L = L_{dyed} - L_{undyed}$, $\Delta a = a_{dyed} - a_{undyed}$, and $\Delta b = b_{dyed} - b_{undyed}$.

The color difference between the largest and the smallest values of the same fabric was obtained, and these values indicate the color evenness of the fabrics. According to the regulation of the National Bureau of Standards (N.B.S.), the fabric is acceptable for use in industrial applications when the color difference is less than 2.0.

Determination of washing fastness

In order to determine the washing fastness, the modified Lyocell fabrics were sewn with cotton fabrics and placed in a steel cylinder. 5 g/L soap, 2 g/L sodium carbonate, 10 stainless steel balls, and 100 mL of aqueous liquid were added to the steel cylinder for each sample. The test temperature was 60 °C and the test time was 30 min. The washing cycle was repeated 10 times. Gray scale was used to assess the grade of color fastness and the extent of color fading.

RESULTS AND DISCUSSION

FTIR analysis of hybrid materials

In the IR spectra of the S_1–S_4 and P_1–P_4 hybrid materials, a strong absorption band in the range from 3414 to 3435 cm^{-1} and 3418 to 3461 cm^{-1}, respectively, dominated. Absorption peaks at approximately 1637-1638 cm^{-1} and 1634-1637 cm^{-1}, respectively, revealed that the hybrid materials had Al–O groups, which enabled the formation of Al–O–Al networks. These results were characteristic of the OH stretching vibrations of free and hydrogen-bonded surface hydroxyl groups.[32,33] Water molecules can be strongly or weakly bound to an alumina surface and form numerous broad OH stretching vibrations. A second typical absorption region for the Si–O stretching vibration of S_1–S_4 and P_1–P_4 at 1035-1038 cm^{-1} and 1032-1038 cm^{-1}, respectively, has been reported. Additionally, the spectrum of Al–O showed doublet absorption bands in the region from 551 to 565 cm^{-1} corresponding to AlO_6 vibrations,[34] thus verifying that the hybrid materials had Al–O groups. In the absorption region at 1271-1285 cm^{-1}, a band due to Si–C bond stretching was found, and the absorption region at 769-776 cm^{-1} was due to deformation of the Si–C bond. Asymmetric stretching vibrations of the C–H bonds in S_1–S_4 and P_1–P_4 were found from 2930 to 2924 cm^{-1} and from 2931 to 2925 cm^{-1}, respectively. Symmetric stretching vibrations of the C–H bonds of S_1–S_4 and P_1–P_4 were found from 2860 to 2854 cm^{-1} and from 2866 to 2858 cm^{-1}, respectively. Thus, it is reasonable to assume that reactions occurred between some of the alumina and silica. Figure 1 shows the FTIR spectra of S_1–S_4. Increasing the OTES concentration increased the strength of the Si–O absorption and strengthened the bonding. Figure 2 shows the FTIR spectra of P_1–P_4. Increasing the alumina concentration increased the strength of the Al–O absorption and also strengthened the bonding. The structures of Si–O–Si and Al–O–Al were also analyzed using ^{29}Si NMR and ^{27}Al NMR.

Analysis of ^{29}Si NMR and ^{27}Al NMR

^{29}Si NMR was used to observe the structure formed by the hydrolysis of Si. While the FTIR results indicate the formation of Si–O–Si by a hydrothermal reaction, ^{29}Si solid-state NMR provides data on the structure of the silica and the extent of the Si–OH condensation reaction.[34] As shown in Figures 3 and 5, the high-resolution solid-state NMR spectra of S_1–S_4 and P_1–P_4, respectively, illustrate absorption peaks at T^3, corresponding to Si–OR, following the hydrolysis of MTMS with OTES, indicating that the absorption structure tended to be of the type $(R–O)Si(–OSi\equiv)_3$. The ^{29}Si NMR spectra of S_1–S_4, shown in Figure 3, indicate that the increase in the molar ratio of OTES under constant molar amounts of AIP and MTMS made the hybrid materials react more completely, so that the absorption peaks of the hybrid materials tend to be smooth, and so the main absorption peaks of the hybrid materials S_1–S_4 tend to be strong. The absorption peak T^3 appeared at approximately −74.21 ppm to −77.58 ppm. The ^{29}Si NMR spectra of P_1–P_4, shown in Figure 5, illustrate the increase in the molar ratio of AIP under constant molar amounts of OTES and MTMS. The results imply that the variation of the T^3 absorption peak tends to be similar to that of S_1–S_4. A single T^3 absorption peak appeared at approximately −75.42 ppm to −77.49 ppm. The Si–O–Si network structure was little affected when the AIP concentration increased. The T^3 absorption peak is merely changed with the higher AIP molar ratio, so that it may be affected by the MTMS or OTES.

According to ^{27}Al-NMR inspection, the coordinate bonds that resulted from the Al hydrolysis were usually 6-coordinate bonds at δ: -10~10 ppm, 5-coordinate bonds at δ: 30~50 ppm, and 4-coordinate bonds at δ: >50 ppm. The ^{27}Al NMR spectra of S_1–S_4 and P_1–P_4 (Figs. 4 and 6, respectively) show that the structure formed during hydrolysis of the chemical precursor aluminum isopropoxide was a six-coordinated alumina with absorption peaks corresponding to literature values in the range from −10 to 10 ppm.

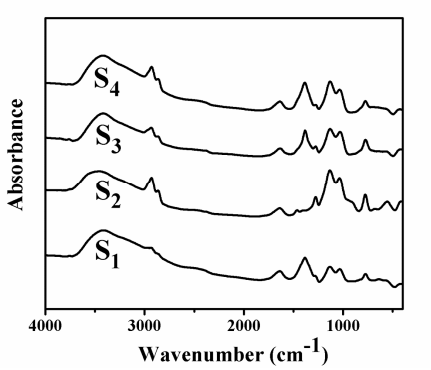

Figure 1: FTIR spectra of S_1–S_4

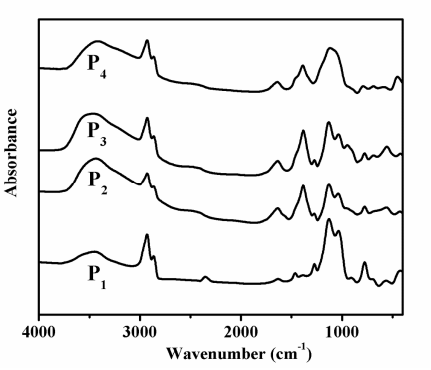

Figure 2: FTIR spectra of P_1–P_4

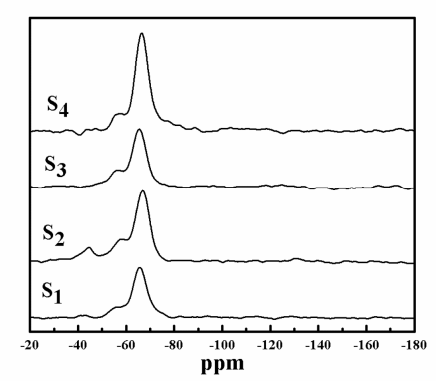

Figure 3: ^{29}Si NMR spectra of S_1–S_4

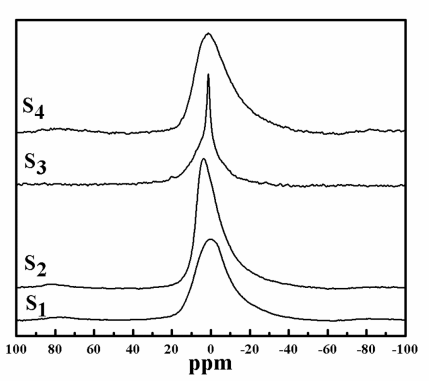

Figure 4: ^{27}Al NMR spectra of S_1–S_4

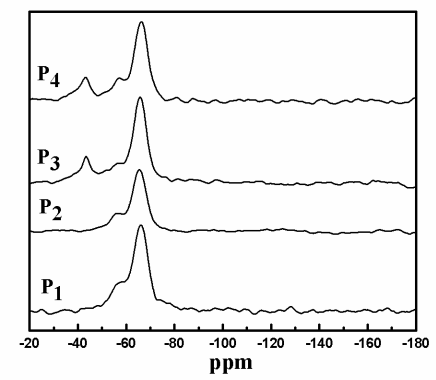

Figure 5: ^{29}Si NMR spectra of P_1–P_4

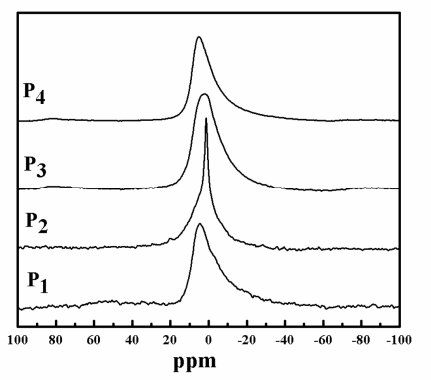

Figure 6: ^{27}Al NMR spectra of P_1–P_4

Table 2
EDS analysis of S_1–S_4 and P_1–P_4

Samples	Elemental composition (%)			
	C	O	Al	Si
S_1	15.64	6.59	14.78	62.99
S_2	15.97	7.01	13.57	63.45
S_3	12.56	7.65	11.75	68.04
S_4	9.55	8.86	11.34	70.25
P_1	17.46	4.76	11.11	66.67
P_2	12.56	7.65	11.75	68.04
P_3	15.24	9.56	23.37	51.83
P_4	22.27	10.26	24.15	43.32

As shown in Figure 4, S_1–S_4 had a single peak at approximately −1.34 ppm to 3.28 ppm, indicative of the hexahedral coordination of Al atoms. As shown in Figure 6, P_1–P_4 had a single peak at approximately 0.84 to 8.43 ppm, which revealed the hexahedral coordination of the Al atoms. As the AIP increased, the six-coordinated alumina absorption peaks tended to higher chemical shift. Moreover, ^{27}Al NMR was used to examine the structure that formed during the hydrolysis of Al, providing additional information about the structure of the alumina and the extent of the Al–OH condensation reaction.

EDS analysis of hybrid materials

Table 2 shows the results of the EDS analyses of S_1–S_4. The molar ratio of the AIP/MTMS/OTES hybrid material increased with increasing amounts of OTES because the $Si(OH)_3$ structure (formed by hydrolysis–condensation of OTES and MTMS) combined with the alumina. The Si peaks revealed that the intensity of the AIP/MTMS/OTES hybrid material increased as the amount of OTES increased. The amounts of carbon and aluminum decreased for the S_4 hybrid material. This was because the S_4 ratio formed more Si–O–Si bonds, which is shown by the high Si content in Figure 7. Furthermore, as seen in Figure 8, the amount of aluminum increased in the P_4-treated Lyocell fabric. Therefore, a larger hybrid material ratio resulted in greater Al–O–Si bonding. According to Table 2, when the MTMS and OTES amounts were fixed, the silica content decreased with increasing aluminum content. The maximum P_4 via AIP addition level in the treated Lyocell fabrics resulted in the maximum aluminum content.

Surface morphology of finished Lyocell fabric

SEM was used to study the morphology of the Lyocell fabrics. The untreated Lyocell fabric shows a smooth morphology (Fig. 9a). SEM micrographs of fabrics treated with varying OTES molar ratios (Fig. 9b-e) show irregularly sized particles with a flake-like morphology. Figure 9b shows small particle blocks and uneven distribution of alumina and silica particles on the surface. As shown in Figure 9c-e, the particle distribution was much more uniform with increasing amounts of silica, indicating that the hybrid materials were more evenly dispersed across the fabric, resulting in the formation of a protective layer. Surface-bound particles were more homogeneous in terms of size and distribution and rough regions appeared on the surface. Fabric pores were marginally filled, resulting in a slight increase in the water repellency characteristics and conductivity. SEM images in Figure 10a-d exhibit fabrics treated with varying AIP molar ratios. An increase in the molar ratio of AIP with constant amounts of OTES and MTMS revealed irregularly sized particles with a flake-like morphology. As the amount of alumina increased, the pore size of the treated surface texture decreased as a result of the Al–O–Al network structure, which effectively filled the pores of the fabrics, thus improving the water repellency characteristics of the treated fabric.

Conductivity of treated Lyocell fabrics

Most fabrics have high surface resistance

and low electrical conductivity, which implies that conductivity and resistance are inversely proportional to each other. As a result, we can measure the resistance of a material to estimate its conductivity. The resistance of gray Lyocell fabrics treated with various hybrid material compositions is shown in Table 3.

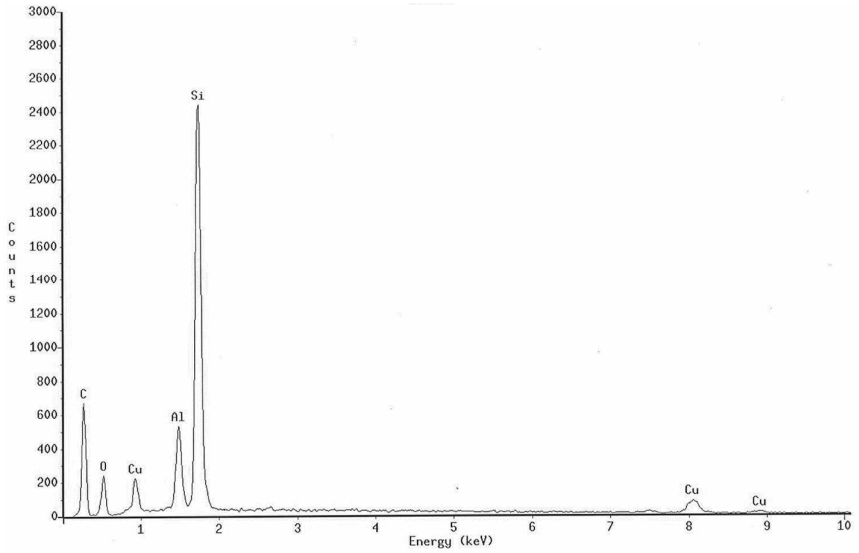

Figure 7: EDS diagram of S_4

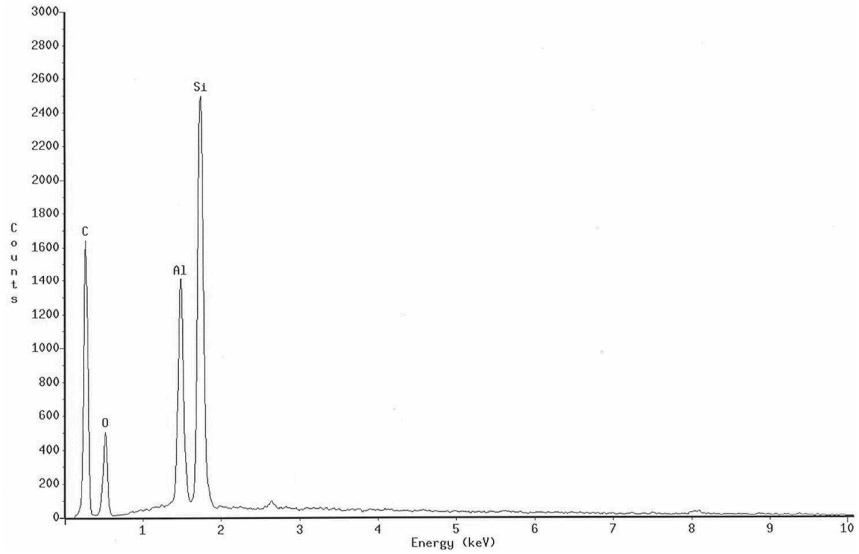

Figure 8: EDS diagram of P_4

Table 3
Conductivity analysis of LS_1–LS_4 and LP_1–LP_4

Compd.	Resistance (Ω)	Compd.	Resistance (Ω)
LS_1	8.72×10^9	LP_1	3.42×10^9
LS_2	2.14×10^8	LP_2	4.86×10^8
LS_3	1.26×10^8	LP_3	8.41×10^8
LS_4	6.42×10^8	LP_4	7.54×10^7

Note: Lyocell fabric is 2.30×10^{10} Ω

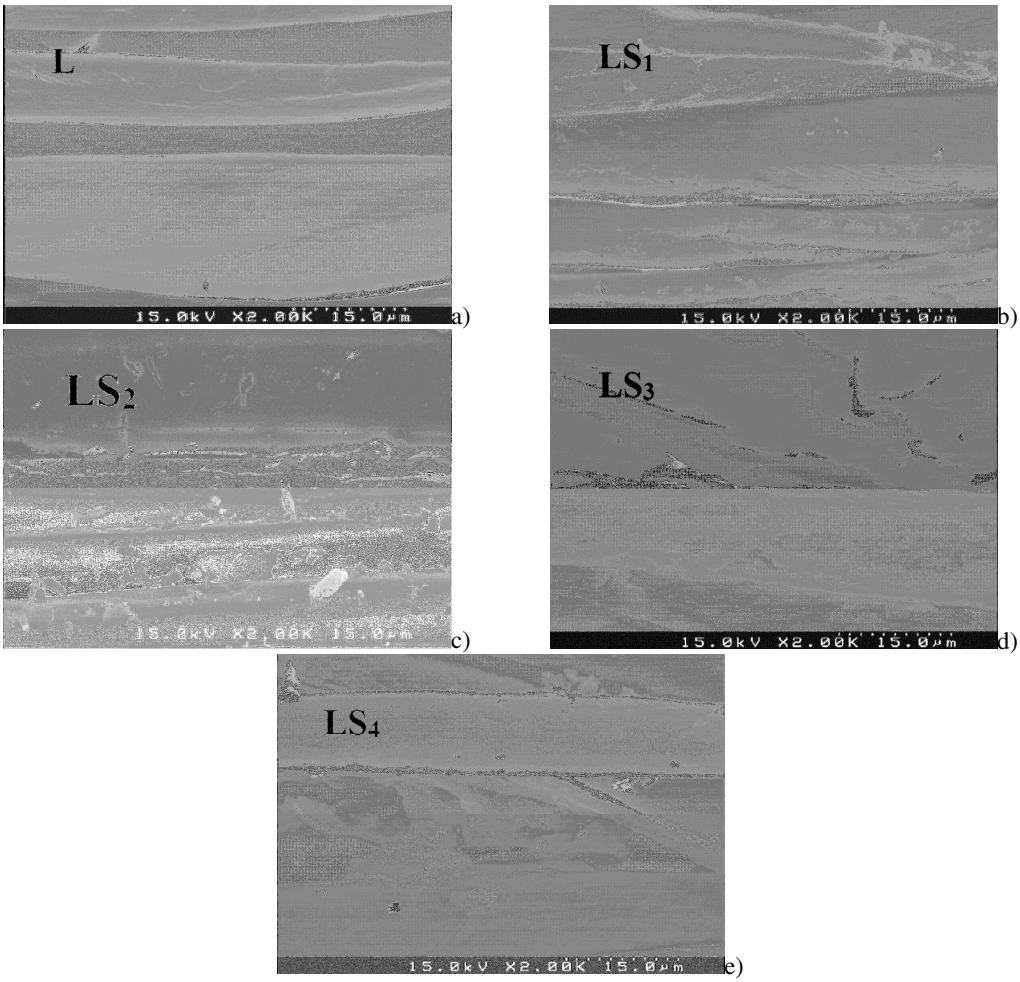

Figure 9: SEM images of untreated (L) and treated (LS_1–LS_4) fabric (×2000)

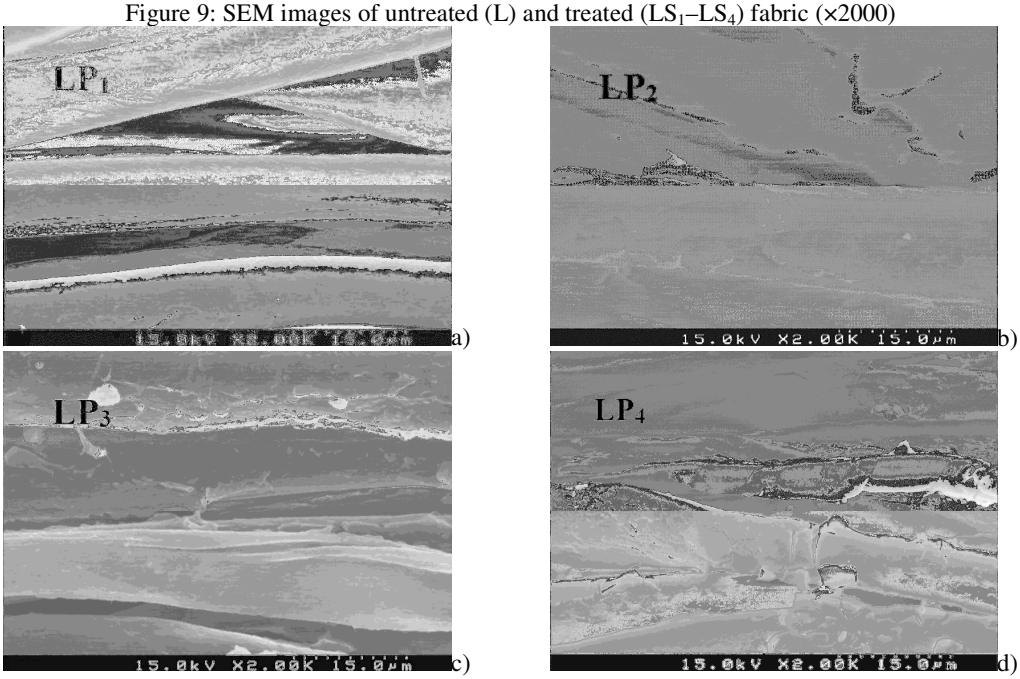

Figure 10: SEM images of LP_1–LP_4 (×2000)

Table 4
Surface hydrophobicity evaluation of LS_1–LS_4 and LP_1–LP_4

Compd.	Contact angle (°)		Compd.	Contact angle (°)	
	Before washing	After washing		Before washing	After washing
Lyocell	0	0	Lyocell	0	0
LS_1	109	104	LP_1	102	95
LS_2	118	107	LP_2	110	101
LS_3	130	117	LP_3	118	107
LS_4	132	116.5	LP_4	121	113

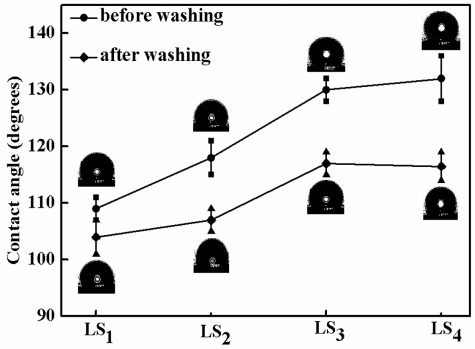

Figure 11: Contact angle analysis of LS_1–LS_4

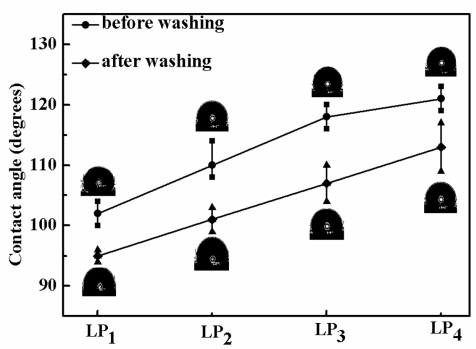

Figure 12: Contact angle analysis LP_1–LP_4

The resistance of the fabrics had an average value of 2.30×10^{10} Ω, indicating that the substrate was non-conductive. The resistance slightly decreased in the range from 6.42×10^8 to 8.72×10^9 Ω for Lyocell fabrics treated with increasing molar ratios of OTES (S_1–S_4). However, the resistance significantly decreased in the range from 7.54×10^7 to 3.42×10^9 Ω for Lyocell fabrics treated with increasing molar ratios of AIP (P_1–P_4). The alumina content significantly enhanced the electric conductivity of the treated fabrics and decreased the resistance by three orders of magnitude at a molar ratio of AIP/MTMS/ OTES of 2:2:2.

Contact angle analysis of treated Lyocell fabrics

Table 4 shows the results of the contact angle analysis for the treated Lyocell fabrics. The contact angle of untreated Lyocell fabrics was 0°. The average contact angle for LS_1 before washing was 109° and this value increased with increasing OTES molar ratio. The increase of OTES molar ratio, in turn, increased the number of siloxane groups in the hybrid materials, which enhanced crosslinking and improved the water repellency characteristics of the Lyocell fabrics. Thus, LS_4 attained the highest contact angle, 132°. The results presented in Figure 12 for the LP_1-LP_4 fabrics show trends similar to those of the LS_1–LS_4 fabrics. However, the contact angles slightly decreased after 10 washing cycles. The reason for these results may be that the hybrid compounds that adhered on the Lyocell fabrics were removed from the surface of the fabrics because of mechanical stirring, thereby negatively affecting the contact angle.

By comparing the contact angles of the LP_1-LP_4 fabrics (Fig. 11), it can be seen that the fabrics treated with LP_4 exhibited the best contact angle of 121°. Further, the dyeing methodology showed little effect on the contact angle of the Lyocell fabrics, as shown in Table 4. The contact angles of LS_4 and LP_4 after washing were 116.5° and 113°, respectively, slightly lower than those of LS_4 and LP_4 before washing

Analysis of color strength and evenness of treated fabrics

Table 5 summarizes the color strength and evenness of the dye of the treated Lyocell

fabrics. LS_1–LS_4 and LP_1–LP_4 showed color strengths ranging from 8.16 to 10.53 K/S. The padding–drying–curing methodology led to poorer penetration of the dye molecules into the fibers, thereby negatively affecting color strength, as shown in Table 5. An increase in the AIP and OTES molar ratios did not improve the color strength and color evenness properties of the treated fabric, as shown in Table 5. The color evenness values were between 0.23 and 0.67, which are within the acceptable range.

Washing color fastness analysis of treated fabrics

Table 6 shows the washing color fastness of the treated Lyocell fabrics. The extent of color fading and staining was grade 4-5 for all of the Lyocell fabrics under study, implying good washing fastness. The bonding forces between the azo dyes and fibers involve hydrogen bonding and van der Waals forces, which are too weak to withstand the washing treatment. However, the crosslinking structures created upon reaction of the dyes with the hybrid materials decisively bound the hybrids tightly on the surface of the Lyocell fabrics, resulting in improved washing fastness properties. The difference in the molar ratios of AIP and OTES did not significantly affect the washing fastness of the fabrics.

Table 5
Color strength and evenness of LS_1–LS_4 and LP_1–LP_4

Compd.	Color strength (K/S)	Evenness (△E)	Compd.	Color strength (K/S)	Evenness (△E)
LS_1	9.25	0.35	LP_1	9.48	0.34
LS_2	8.47	0.24	LP_2	8.35	0.57
LS_3	8.41	0.65	LP_3	8.26	0.39
LS_4	8.28	0.58	LP_4	8.13	0.27

Table 6
Washing color fastness of LS_1–LS_4 and LP_1–LP_4

Compd.	Washing		Compd.	Washing	
	Fading	Staining		Fading	Staining
LS_1	5	4–5	LP_1	4–5	4–5
LS_2	5	5	LP_2	4–5	4–5
LS_3	5	4–5	LP_3	5	5
LS_4	5	5	LP_4	5	5

CONCLUSION

Alumina/silica hybrid materials were synthesized using a hydrothermal process with various molar ratios of the aluminum isopropoxide and OTES chemical precursors. The properties of Lyocell fabrics coated with the AIP/MTMS/OTES hybrid materials were examined, and FTIR, ^{27}Al NMR, ^{29}Si NMR, and EDS analyses confirmed that the alumina and silica in the hybrid materials bonded to form a network. The FTIR spectra indicated increasing numbers of Si–O–Si and Al–O–Al linkages as the molar ratios of AIP and OTES increased. Thus, the addition of adequate amounts of AIP/MTMS/OTES can improve the water repellency properties of treated Lyocell fabrics, as indicated by the contact angle results for untreated Lyocell fabrics (0°) and treated fabrics (109–132°). It was also found that the difference in the molar ratios of AIP and OTES did not significantly affect the washing fastness of the fabrics. However, an increase in the alumina content significantly enhanced the electric conductivity of the treated fabrics and decreased the resistance by three orders of magnitude at AIP/MTMS/OTES molar ratios of 2:2:2.

ACKNOWLEDGMENTS: The authors would like to thank the National Science Council of

the Republic of China, Taiwan, for financially supporting this research under grant NSC 100-2622-E-168- 007-CC3.

REFERENCES

[1] T. Rosenau, A. Hofinger, A. Potthast and P. Kosma, *Polymer*, **44**, 6153 (2003).
[2] C. Woodings, "Regenerated Cellulose Fibers", Woodhead Publishing Ltd., Cambridge, England, 2001, p. 62.
[3] X. P. Zhuang, X. F. Liu, S. Y. Li, B. W. Cheng and W. M. Kang, *Fiber. Polym.*, **9**, 400 (2008).
[4] P. L. Nostro, D. Corrieri, M. Ceccato and P. Baglioni, *J. Colloid. Interf. Sci.*, **236**, 270 (2001).
[5] S. M. Burkinshaw and R. Krishna, *Dyes Pigments.*, **27**, 113 (1995).
[6] N. Veronovski and M. Sfiligoj-Smole, *Fiber. Polym.*, **11**, 545 (2010).
[7] T. Matsuo, *Text. Prog.*, **40**, 123 (2008).
[8] H. Y. Ki, J. H. Kim, S. C. Kwon and S. H. Jeong, *J. Mater. Sci.*, **42**, 8020 (2007).
[9] K. Qi, J. H. Xin, W. A. Daoud and C. L. Mak, *Int. J. Appl. Ceram. Technol.*, **4**, 554 (2007).
[10] R. Kotek, *Polym. Rev.*, **48**, 221 (2008).
[11] C. Sanchez, B. Julian, P. Belleville and M. Popall, *J. Mater. Chem.*, **15**, 3559 (2005).
[12] A. Morales and A. Duran, *J. Sol-Gel Sci. Techn.*, **8**, 451 (1997).
[13] Y. Kurokawa, T. Shirakawa, S. Saito and N. Yui, *J. Mater. Sci. Lett.*, **5**, 1070 (1986).
[14] Y. C. Chen, X. Ai, C. Z. Hueng and B. Y. Wang, *Mater. Sci. Techn.*, **288**, 19 (2000).
[15] B. E. Yoldas, *Am. Ceram. Soc. Bull.*, **54**, 289 (1975).
[16] J. Chandradass and M. Balasubramanian, *J. Mater. Sci.*, **41**, 6026 (2006).
[17] Z. Wen, E. M. James, R. U. Marilyn and E. A. Fred, *J. Appl. Polym. Sci.*, **79**, 2326 (2001).
[18] C. Anderson and A. J. Bard. *J. Phys. Chem.*, **99**, 9882 (1995).
[19] O. Kesmez, H. E. Camurlu, E. Burunkaya and E. Arpac, *Sol. Energ. Mat. Sol. C.*, **93**, 1833 (2009).
[20] M. Houmard, D. Riassetto, F. Riassetto, A. Bourgeois, G. Berthome *et al.*, *Appl. Surf. Sci.*, **254**, 1405 (2007).
[21] S. J. Khatib and S. T. Oyama, *Sep. Purif. Technol.*, **111**, 20 (2013).
[22] J. Zhu, B. Y. Tay and J. Ma, *J. Mater. Process. Tech.*, **192–193**, 561 (2007).
[23] K. Byrappa, A. K. Subramani, S. Ananda, K. M. L. Rai, M. H. Sunitha *et al.*, *J. Mater. Sci.*, **41**, 1355 (2006).
[24] S. Y. Wu, W. Zhang and X. M. Chen, *J. Mater. Sci. Mater. El.*, **21**, 450 (2010).
[25] Z. Hui, L. Fang and Z. Hong, *Fiber. Polym.*, **14**, 43 (2013).
[26] J. Choi, S. Komarneni, K. Grover, H. Katsuki and M. Park, *Appl. Clay Sci.*, **46**, 69 (2009).
[27] R. Pazik, D. Hreniak and W. Strek, *Mater. Res. Bull.*, **42**, 1188 (2007).
[28] Y. Q. Wang, J. F. Huang, Z. H. Chen and L. Y. Cao, *J. Compos. Mater.*, **46**, 409 (2011).
[29] X. Wu, B. Zhang and Z. Hu, *Mater. Lett.*, **73**, 169 (2012).
[30] T. Mousavand, S. Ohara, M. Umetsu, J. Zhang, S. Takami *et al.*, *J. Supercrit. Fluid.*, **40**, 397 (2007).
[31] V. R. G. Dev, J. Venugopal, S. Sudha, G. Deepika and S. Ramakrishna, *Carbohyd. Polym.*, **75**, 646 (2009).
[32] M. C. Canela, R. M. Alberici and W. F. Jardim, *J. Photoch. Photobio. C.*, **112**, 73 (1998).
[33] I. M. Low and R. McPherson, *J. Mater. Sci.*, **24**, 892 (1989).
[34] R. J. Hook, *J. Non-Cryst. Solids.*, **195**, 1 (1996).